

Rotation symmetry breaking in $\text{La}_{2-x}\text{Sr}_x\text{CuO}_4$ revealed by angle-resolved photoemission spectroscopy

E. Razzoli,^{1,2,*} C. E. Matt,^{1,3} Y. Sassa,^{1,3,4} M. Månsson,^{5,6,7} O. Tjernberg,⁷ G. Drachuck,⁸ M. Monomo,⁹ M. Oda,¹⁰ T. Kurosawa,¹⁰ Y. Huang,¹¹ N. C. Plumb,¹ M. Radovic,¹ A. Keren,⁸ L. Patthey,¹ J. Mesot,^{1,3,12} and M. Shi¹

¹Swiss Light Source, Paul Scherrer Institute, CH-5232 Villigen PSI, Switzerland

²Département de Physique and Fribourg Center for Nanomaterials, Université de Fribourg, CH-1700 Fribourg, Switzerland

³Laboratory for Solid State Physics, ETH Zurich, CH-8093 Zurich, Switzerland

⁴Department of Physics and Astronomy, Uppsala University, S-75121 Uppsala, Sweden

⁵Laboratory for Quantum Magnetism (LQM), Ecole Polytechnique Fédérale de Lausanne (EPFL), Station 3, CH-1015 Lausanne, Switzerland

⁶Laboratory for Neutron Scattering, Paul Scherrer Institut, CH-5232 Villigen PSI, Switzerland

⁷KTH Royal Institute of Technology, Materials Physics, Electrum 229, 164 40 Kista, Stockholm, Sweden

⁸Physics Department, Technion, Israel Institute of Technology, Haifa 32000, Israel

⁹Department of Applied Sciences, Muroran Institute of Technology, Muroran 050-8585, Japan

¹⁰Department of Physics, Hokkaido University, Sapporo 060-0810, Japan

¹¹Beijing National Laboratory for Condensed Matter Physics, and Institute of Physics, Chinese Academy of Sciences, Beijing 100190, China

¹²Institut de la Matière Complexe, EPF Lausanne, CH-1015, Lausanne, Switzerland

(Received 7 May 2014; revised manuscript received 16 May 2017; published 7 June 2017)

Using angle-resolved photoemission spectroscopy it is revealed that in the vicinity of optimal doping the electronic structure of $\text{La}_{2-x}\text{Sr}_x\text{CuO}_4$ cuprate undergoes an electronic reconstruction associated with a wave vector $\mathbf{q}_a = (\pi, 0)$. The reconstructed Fermi surface and folded band are distinct to the shadow bands observed in BSCCO cuprates and in underdoped $\text{La}_{2-x}\text{Sr}_x\text{CuO}_4$ with $x \leq 0.12$, which shift the primary band along the zone diagonal direction. Furthermore, the folded bands appear only with $\mathbf{q}_a = (\pi, 0)$ vector, but not with $\mathbf{q}_b = (0, \pi)$. We demonstrate that the absence of \mathbf{q}_b reconstruction is not due to the matrix-element effects in the photoemission process, which indicates the fourfold symmetry is broken in the system.

DOI: [10.1103/PhysRevB.95.224504](https://doi.org/10.1103/PhysRevB.95.224504)

I. INTRODUCTION

Since the discovery of high-temperature cuprate superconductors, the study of various instabilities (e.g., magnetic and charge order) emerging in close proximity to superconductivity has attracted much attention. Significant efforts have been devoted to reveal other instabilities than the superconducting one, as a function of doping and temperature, and how they are intertwined with the superconductivity. Recently, an incipient incommensurate charge-density-wave (CDW) in underdoped $\text{YBa}_2\text{Cu}_3\text{O}_{6+y}$ (YBCO) with hole concentrations in the range of 0.09 to 0.13 per planar Cu ion has been reported independently from high-energy x-ray diffraction [1] and resonant soft x-ray scattering [2] experiments. Similar charge modulations along the Cu-O bonding directions of underdoped $\text{Bi}_2\text{Sr}_{2-x}\text{La}_x\text{CuO}_{6+\delta}$ (Bi2201) and $\text{Bi}_2\text{Sr}_2\text{CaCu}_2\text{O}_{8+\delta}$ (Bi2212) have also been observed in scanning-tunneling microscopy and resonant x-ray scattering measurements, with the ordering vector approaching a commensurate wave vector $(0.25 \times \pi/a)$ when the hole doping is increasing [3,4]. For the underdoped La-based “214” family of cuprates $[\text{La}_{2-x-y}(\text{Sr},\text{Ba})_x(\text{Nd},\text{Eu})_y\text{CuO}_4]$ at a doping level $x \approx 1/8$, a unidirectional modulated antiferromagnetism [5] combined with a commensurate charge modulation of period four lattice constants (stripe order) has long been identified, and at the same doping level the superconducting transition

temperature is dramatically reduced [6,7]. The presence of stripe order in $\text{La}_{2-x}\text{Sr}_x\text{CuO}_4$ has been debated for long time and only recently scattering measurements have shown evidence for a CDW with a wave vector \mathbf{q} displaying a doping dependence similar to the one observed in Bi2201 and $\text{La}_{2-x}\text{Ba}_x\text{CuO}_4$ [8–10]. However, so far, angle-resolved photoemission spectroscopy (ARPES) measurements have not shown any evidence of band folding associated with charge ordering along the Cu-O bond direction in cuprates [11–13].

In this letter, applying ARPES to nearly optimally doped LSCO ($x = 0.15, 0.17$) we show that in the superconducting phase the Fermi surface (FS) is reconstructed along the Cu-O bond direction associated with a wave vector $\mathbf{q}_a = (\pi, 0)$. This wave vector could be related to the second harmonic of an incipient CDW in the region of optimal doping, which is the smooth continuation with doping of the incipient CDW as observed in other cuprates, or could point to a new instability in the system.

II. EXPERIMENTAL DETAILS

ARPES experiments were carried out at the Surface and Interface Spectroscopy beamline at the Swiss Light Source of Paul Scherrer institute on single crystals $\text{La}_{2-x}\text{Sr}_x\text{CuO}_4$ (LSCO). The doping values used for the measurements are $x = 0.15$ and 0.17 with superconducting transition temperature T_c of 38 and 35 K, respectively. The crystals were grown in traveling solvent floating zone furnaces. All samples were characterized by x-ray diffraction, and their superconducting transitions were determined by magnetization measurements.

*Present address: Quantum Matter Institute, Department of Physics and Astronomy, University of British Columbia, Vancouver, British Columbia V6T 1Z1, Canada.

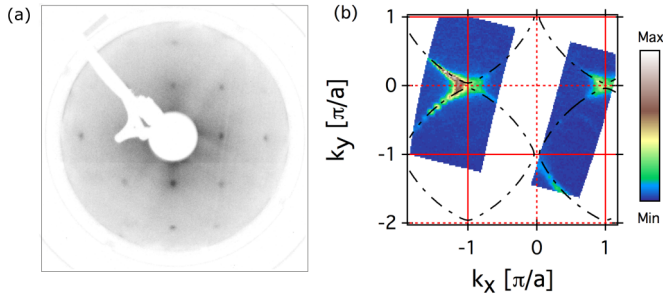


FIG. 1. (a) LEED pattern taken at $T = 12$ K and $E_e = 185$ eV. (b) FS mapping for LSCO $x = 0.17$. Dashed-pointed black line is a TB fit as explained in the text.

Circularly polarized light with $h\nu = 55$ eV was used in order to maximize the signal. The spectra were recorded with Scienta R4000 analyzers. The energy and angle resolutions were ~ 15 meV and 0.1° – 0.15° , respectively. The Fermi level was determined by recording photoemission spectra from polycrystalline copper on the sample holder. The samples were cleaved in situ by using a specially designed cleaver [14]. Low-energy electron diffraction analysis of the cleaved samples shows a clear (1×1) pattern with no sign of surface reconstruction [see Fig. 1(a)]. During the measurements, the base pressure always remained less than 5×10^{-11} mbar.

III. EXPERIMENTAL RESULTS

Figure 1(b) shows the spectral weight mapping in k space at Fermi level (E_F). The superimposed dashed black line is the FS obtained from a tight-binding (TB) fit to the k_F extracted from the peak positions of momentum distribution curves (MDC) at E_F and to the MDC peak positions, as a function of binding energy, along the zone diagonal (nodal dispersion). The basis functions and the obtained fitting coefficients with the constraint $t_3/t_2 = -1/2$ [15] are listed in Table I. Luttinger sum rule [16] gives a hole concentration of $x \sim 0.19$, slightly bigger than the nominal doping $x = 0.17$, in agreement with the observation in early studies [17].

To enhance the weak features, in Fig. 2(a), we display the intensity map at E_F in logarithmic color scale. Besides the primary FS in map I, in the middle of the intensity plot [see also Fig. 1(b)], two weak but clearly visible pieces of FS appear on the left and right sides of the primary FS. In Fig. 2(b), we plot the k_F extracted from the peak positions in map I of MDC at E_F for both the primary FS (red triangles) and the weak pieces of FS (blue circles). It can be seen that the two weak pieces of FS mirror the primary FS about the

TABLE I. Tight-binding coefficient and basis functions used in fitting the experimental data. The second column lists the coefficient of each term (meV) following the convention: $\epsilon(\mathbf{k}) = \sum t_i \eta_i(\mathbf{k})$.

i	t_i	$\eta_i(\mathbf{k})$
0	134	1
1	181	$-2[\cos(k_x a) + \cos(k_y a)]$
2	-23	$-4[\cos(k_x a) \cos(k_y a)]$
3	12	$-2[\cos(2k_x a) + \cos(2k_y a)]$

vertical lines at $k_x = \pm\pi/2$, which is equivalent to shifting the primary FS by a commensurate wave vector $\mathbf{q}_a = (\pi, 0)$ (dashed violet line). The appearance of the weak pieces of FS indicates that a Fermi surface reconstruction related to a wave vector \mathbf{q}_a occurs in the system. The reconstructed FS is different to the shadow FS previously observed in LSCO [18,19] and in BSCCO cuprates [20] because in those cases the shadow FS is connected to the primary FS by a wave vector along the zone diagonal, i.e., in the (π, π) direction. It is important to mention that we have observed a reconstructed FS related to the wave vector $\mathbf{q}_a = (\pi, 0)$, which is nearly parallel to the cut direction, but found no sign for a reconstruction corresponding to wave vector $\mathbf{q}_b = (0, \pi)$. The lack of the \mathbf{q}_b -folded band might be due to two different effects; the \mathbf{q}_b folded band is present but not observed due to ARPES selection rules (the so-called “matrix element effects”) [21] or the this folded band is not present and the C_4 rotational symmetry of the system is broken in favor of C_2 symmetry. To confirm that the lack of \mathbf{q}_b reconstruction is not due to the matrix element effects in the photoemission process, we rotated the sample about the surface normal (c axis) by 90° and acquired ARPES data with otherwise unchanged experimental conditions. In case of matrix element effects, we would expect to see the band folded again in a direction parallel to the (new) cut direction, i.e., along the $(0, \pi) = \mathbf{q}_b$. As shown in map II of Fig. 2(a) and in the corresponding k_F in Fig. 2(b) (light-blue pentagons and green rhombus), the reconstructed FS is not displaced along \mathbf{q}_b but still follows the original folding direction \mathbf{q}_a . This observation demonstrates that the reconstruction of FS is not due to matrix element effects and it ascertains that the fourfold symmetry is broken in the system. The \mathbf{q}_a reconstruction is further illustrated in Fig. 3, which shows the band dispersions along cut 1–4 as indicated in Fig. 2(b). All the folded bands associated with the reconstruction can be reproduced after shifting the primary band by a wave vector \mathbf{q}_a . On the other hand, no folded band related to \mathbf{q}_b reconstruction was observed.

We have investigated the folded bands in LSCO in a wide doping range. For $x \leq 0.12$, a folded band related to a shifting of the primary band by $\mathbf{q} = (\pi, \pi)$ was observed [19]. For $x \geq 0.22$, except the primary FS and band, there is no indication for any observable reconstructed FS and folded band in our ARPES data acquired in the same experimental conditions. The $\mathbf{q}_a = (\pi, 0)$ FS reconstruction and the associated band folding appear only in the vicinity of optimally doped samples ($x = 0.15, 0.17$). Figure 4 shows the ARPES spectra taken from a slightly underdoped LSCO sample with $x = 0.15$. Although the intensity is weaker than the case for $x = 0.17$, the folded bands are still clearly visible, as indicated by the arrows in Figs. 4(a)–4(e). The k_F extracted from the peak positions of MDC at E_F show that the folded bands and their FS result from a $\mathbf{q}_a = (\pi, 0)$ reconstruction [Fig. 4(f)].

IV. DISCUSSION

The $\mathbf{q}_a = (\pi, 0)$ electronic reconstruction in the vicinity of optimal doping of LSCO ($x = 0.15, 0.17$) is different to the previously observed shadow bands and FS duplication along the zone diagonal in cuprates [18–20]. This rules out the possibility that the $\mathbf{q}_a = (\pi, 0)$ reconstruction is due to

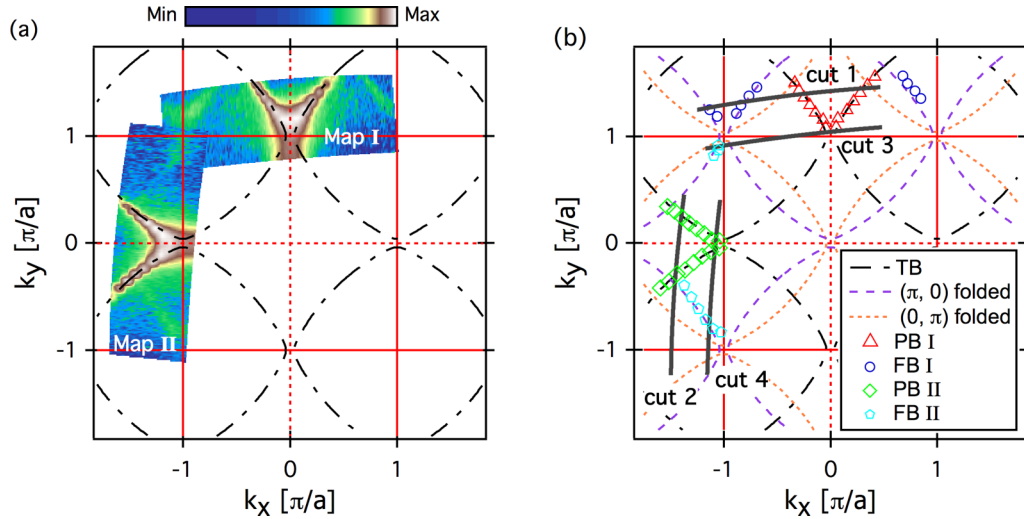


FIG. 2. ARPES Intensity plots of $\text{La}_{2-x}\text{Sr}_x\text{CuO}_4$ ($x = 0.17$). The data were taken at 12 K. (a) FS intensity maps in the $k_x - k_y$ plane at $h\nu = 55$ eV and $T = 12$ K. Map II is the same as Map I but after a 90° rotation of the sample. The FS maps in I-II are obtained by integrating ARPES spectral weight in an energy window of $E_F \pm 20$ meV. (b) Red triangles (green rombus) and blue circles (light-blue pentagons) are the k_F for the primary band (PB) and the folded band (FB) extracted from the MDCs peaks for the sample oriented like in map I (map II), respectively. Dashed-pointed black line is a TB fit to the PB data, dashed violet line is the TB FS shifted by $\mathbf{q}_a = (\pi, 0)$, and dotted orange line is the TB FS shifted by $\mathbf{q}_b = (0, \pi)$.

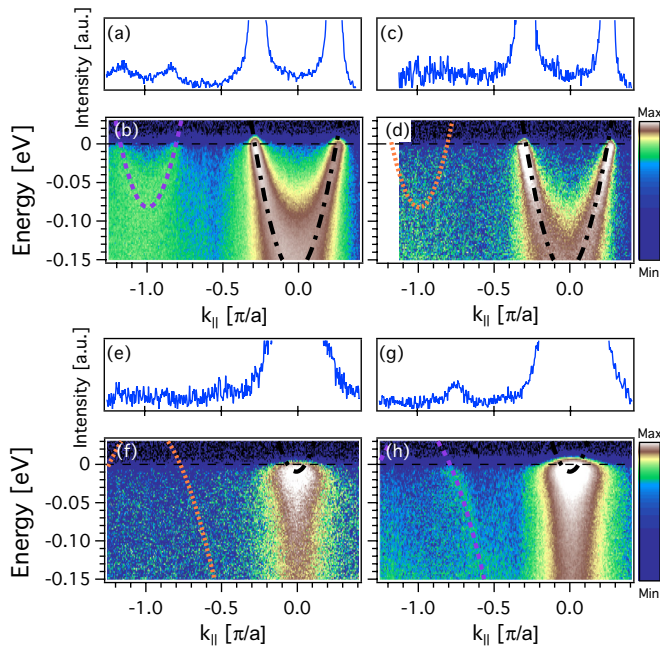


FIG. 3. Dispersion of the primary and folded band along selected cuts for $\text{La}_{2-x}\text{Sr}_x\text{CuO}_4$ ($x = 0.17$). The data were taken at 12 K. (a) and (b) MDC at the $E_F - 0.01$ meV and ARPES intensity map for the cut 1 in Fig. 2(c), respectively. (c) and (d) MDC at the $E_F - 0.01$ meV and ARPES intensity map for the cut 2 in Fig. 2(d), respectively. (e) and (f) MDC at the $E_F - 0.01$ meV and ARPES intensity map for the cut 3 in Fig. 2(c), respectively. (g) and (h) MDC at the $E_F - 0.01$ meV and ARPES intensity map for the cut 4 in Fig. 2(d), respectively. The dispersions of the bands folded by $\mathbf{q}_a = (\pi, 0)$ (dashed violet line) and $\mathbf{q}_b = (0, \pi)$ (dotted orange line) are superimposed to the intensity maps in (b), (h) and (d), (f), respectively.

structurally orthorhombic distortions (LTO) of the crystal structure from tetragonality, because in that case one would expect that a copy of the primary FS is shifted along the (π, π) direction [22]. A low temperature tetragonal reconstruction (LTT), as the one observed in $\text{La}_{2-x}\text{Ba}_x\text{CuO}_4$ [23], localized at the surface of LSCO could explain the $(\pi - 0)$ reconstruction.

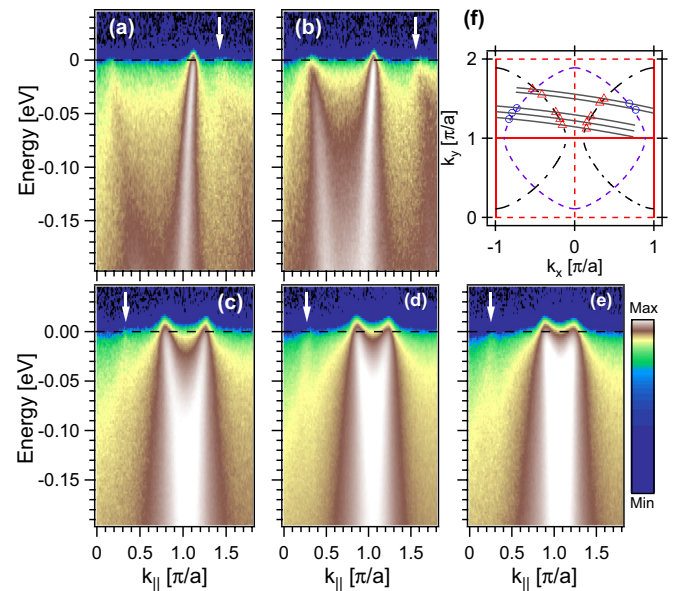


FIG. 4. (a)–(e) ARPES Intensity plots of $\text{La}_{2-x}\text{Sr}_x\text{CuO}_4$ ($x = 0.15$) along the cuts (from top to bottom) shown in (f). The data were taken at 12 K. White arrows indicate the folded band. (f) Black curves are FS of the primary band. The violet curve is a copy of the primary FS, but shifted by $\mathbf{q}_a = (\pi, 0)$. Black lines indicate the momentum cuts. Red triangles and blue empty circles are k_F of the primary and the folded bands, which are determined from MDCs at zero binding energy.

Indeed, LSCO has been reported to be on the verge of an LTO to LTT transition at low temperature [24], which could get stabilized at the surface during the cleaving procedure. However, while our measurements report that the $(\pi - 0)$ reconstruction is stabilized only in a narrow range of optimal dopings ($x = 0.15 - 0.17$), inelastic neutron-scattering measurements show that at the LTO-LTT structure instability is stronger at low dopings ($x \leq 0.12$) [25]. The opposite dependence of the LTO-LTT instability and of the reported $(\pi - 0)$ folding suggests that the two effects may not be related. The absence in the LEED patterns [see, e.g., Fig. 1(a)] of any signature of 1×2 or 2×1 surface reconstruction indicates that the folding could result from a dynamic charge modulation or from a nontrivial structural distortion, similar but different to the case of Bi2212 shadow bands [22], where an orthorhombic distortion was observed in LEED only at very low energies (below 20 eV) [26].

The strong doping dependence of the folded bands suggests that the folding, independently from its origin, is somehow tied to the electronic properties of the sample. The \mathbf{q}_a folded bands were observed at $T = 12$ K, which is well below the superconducting temperature 38 and 35 K for LSCO with $x = 0.15$ and 0.17, respectively. This suggests that if the \mathbf{q}_a electronic reconstruction is associated with an instability in the system such as a density wave, the ordering coexists with superconducting instability. We note that the \mathbf{q}_a wave vector associated with the electronic reconstruction is unexpected from the smooth continuation of the incipient incommensurate charge-density-wave along the Cu-O bonding direction, observed in LSCO [8–10] and other underdoped cuprates [1–4]. There, with increasing doping, the incipient incommensurate wave vector is approaching a commensurate one $(\pi/2, 0)$, instead of $\mathbf{q}_a = (\pi, 0)$. However, one possibility could be that the observed \mathbf{q}_a corresponds to band folding associated with two times of $(\pi/2, 0)$, and the electronic states related to the $(\pi/2, 0)$ reconstruction are too weak to be observed due to the matrix element effects in the photoemission process. Another possibility is that the \mathbf{q}_a reconstructed FS is related the change of FS topology near $x = 0.17$ [19]. In LSCO, at a doping level slightly above $x = 0.17$, the primary FS changes from a holelike pocket centered at the (π, π) point to an electronlike

pocket centered at the Γ point, the center of the BZ. Accompanying the topological change of the FS, a Van Hove singularity at $(\pi, 0)$ saddle-point approaches the Fermi level. The large and discontinuous density of states near E_F could result in a dynamic charge modulation, which leads to a spontaneous breakdown of the point group symmetry [27,28]. The charge modulations could involve the whole crystal or the bulk system could be on the verge of a $(\pi, 0)$ electronic reconstruction, which gets stabilized only at the surface by the disorder and/or the breaking of translational symmetry, similarly to what was shown for the stripe order in LSCO with $x = 1/8$ [29].

Regardless of the exact origin, our observation indicates that at low temperatures an instability associated with the breaking of C_4 symmetry coexists with superconductivity near the optimal doping of LSCO. However, it is unclear whether the observed $\mathbf{q}_a = (\pi, 0)$ electronic reconstruction is general for hole-doped superconducting cuprates, or is particularly related to LSCO.

V. CONCLUSIONS

In summary, using ARPES we revealed the presence of a weaker folded band, which resembles the primary band shifted by $\mathbf{q}_a = (\pi, 0)$ in the superconducting state of nearly optimally doped LSCO ($x = 0.15, 0.17$). We show that the absence of a $\mathbf{q}_b = (0, \pi)$ folded band is intrinsic but not due to the matrix element effects of the photoemission process, which indicates that the C_4 symmetry is broken in the system. The unusual doping dependence of such folded bands deserves further study to identify its origin.

ACKNOWLEDGMENTS

We are grateful to J. Chang for useful discussions. This work was performed at SLS of the Paul Scherrer Institut, Villigen PSI, Switzerland and it was supported by the Swiss National Science Foundation through NCCR MaNEP and the Grant No. 200021-137783. E.R. acknowledges support from the Swiss National Science Foundation (SNSF) Grant No. P300P2_164649. M.M. and Y.S. acknowledge project funding from the Swedish Research Council (Dnr. 2016-06955). We thank the beam line staff of SIS for their excellent support.

-
- [1] J. Chang, E. Blackburn, A. T. Holmes, N. B. Christensen, J. Larsen, J. Mesot, R. Liang, D. A. Bonn, W. N. Hardy, A. Watenphul, M. v. Zimmermann, E. M. Forgan, and S. M. Hayden, *Nat. Phys.* **8**, 871 (2012).
 - [2] G. Ghiringhelli, M. Le Tacon, M. Minola, S. Blanco-Canosa, C. Mazzoli, N. B. Brookes, G. M. De Luca, A. Frano, D. G. Hawthorn, F. He, T. Loew, M. Moretti Sala, D. C. Peets, M. Salluzzo, E. Schierle, R. Sutarto, G. A. Sawatzky, E. Weschke, B. Keimer, and L. Braicovich, *Science* **337**, 821 (2012).
 - [3] R. Comin, A. Frano, M. M. Yee, Y. Yoshida, H. Eisaki, E. Schierle, E. Weschke, R. Sutarto, F. He, A. Soumyanarayanan, Y. He, M. Le Tacon, I. S. Elfimov, J. E. Hoffman, G. A. Sawatzky, B. Keimer, and A. Damascelli, *Science* **343**, 390 (2014).
 - [4] E. H. da Silva Neto, P. Aynajian, A. Frano, R. Comin, E. Schierle, E. Weschke, A. Gyenis, J. Wen, J. Schneeloch, Z. Xu, S. Ono, G. Gu, M. Le Tacon, and A. Yazdani, *Science* **343**, 393 (2014).
 - [5] M. Platé, J. D. F. Mottershead, I. S. Elfimov, D. C. Peets, R. Liang, D. A. Bonn, W. N. Hardy, S. Chiuzaibaian, M. Falub, M. Shi, L. Patthey, and A. Damascelli, *Phys. Rev. Lett.* **95**, 077001 (2005).
 - [6] J. M. Tranquada, B. J. Sternlieb, J. D. Axe, Y. Nakamura, and S. Uchida, *Nature (London)* **375**, 561 (1995).
 - [7] J. M. Tranquada, J. D. Axe, N. Ichikawa, Y. Nakamura, S. Uchida, and B. Nachumi, *Phys. Rev. B* **54**, 7489 (1996).
 - [8] T. P. Croft, C. Lester, M. S. Senn, A. Bombardi, and S. M. Hayden, *Phys. Rev. B* **89**, 224513 (2014).
 - [9] N. B. Christensen, J. Chang, J. Larsen, M. Fujita, M. Oda, M. Ido, N. Momono, E. M. Forgan, A. T. Holmes, J. Mesot, M. Huecker, and M. v. Zimmermann, [arXiv:1404.3192](https://arxiv.org/abs/1404.3192).
 - [10] V. Thampy, M. P. M. Dean, N. B. Christensen, L. Steinke, Z. Islam, M. Oda, M. Ido, N. Momono, S. B. Wilkins, and J. P. Hill, *Phys. Rev. B* **90**, 100510 (2014).

- [11] Y. Kohsaka, C. Taylor, P. Wahl, A. Schmidt, J. Lee, K. Fujita, J. W. Alldredge, K. McElroy, J. Lee, H. Eisaki, S. Uchida, D.-H. Lee, and J. C. Davis, *Nature (London)* **454**, 1072 (2008).
- [12] J. Meng, G. Liu, W. Zhang, L. Zhao, H. Liu, X. Jia, D. Mu, S. Liu, X. Dong, J. Zhang, W. Lu, G. Wang, Y. Zhou, Y. Zhu, X. Wang, Z. Xu, C. Chen, and X. J. Zhou, *Nature (London)* **462**, 335 (2009).
- [13] A. Kanigel, M. R. Norman, M. Randeria, U. Chatterjee, S. Souma, A. Kaminski, H. M. Fretwell, S. Rosenkranz, M. Shi, T. Sato, T. Takahashi, Z. Z. Li, H. Raffy, K. Kadowaki, D. Hinks, L. Ozyuzer, and J. C. Campuzano, *Nat. Phys.* **2**, 447 (2006).
- [14] M. Månsson, T. Claesson, U. O. Karlsson, O. Tjernberg, S. Pailh s, J. Chang, J. Mesot, M. Shi, L. Patthey, N. Momono, M. Oda, and M. Ido, *Rev. Sci. Instr.* **78**, 076103 (2007).
- [15] E. Pavarini, I. Dasgupta, T. Saha-Dasgupta, O. Jepsen, and O. K. Andersen, *Phys. Rev. Lett.* **87**, 047003 (2001).
- [16] J. M. Luttinger, *Phys. Rev.* **119**, 1153 (1960).
- [17] T. Yoshida, X. J. Zhou, K. Tanaka, W. L. Yang, Z. Husain, Z.-X. Shen, A. Fujimori, S. Sahrakorpi, M. Lindroos, R. S. Markiewicz, A. Bansil, S. Komiya, Y. Ando, H. Eisaki, T. Kakeshita, and S. Uchida, *Phys. Rev. B* **74**, 224510 (2006).
- [18] J. Chang, Y. Sassa, S. Guerrero, M. Månsson, M. Shi, S. Pailh s, A. Bendounan, R. Mottl, T. Claesson, O. Tjernberg, L. Patthey, M. Ido, M. Oda, N. Momono, C. Mudry, and J. Mesot, *New J. Phys.* **10**, 103016 (2008).
- [19] E. Razzoli, Y. Sassa, G. Drachuck, M. Månsson, A. Keren, M. Shay, M. H. Berntsen, O. Tjernberg, M. Radovic, J. Chang, S. Pailh s, N. Momono, M. Oda, M. Ido, O. J. Lipscombe, S. M. Hayden, L. Patthey, J. Mesot, and M. Shi, *New J. Phys.* **12**, 125003 (2010).
- [20] P. Aebi, J. Osterwalder, P. Schwaller, L. Schlapbach, M. Shimoda, T. Mochiku, and K. Kadowaki, *Phys. Rev. Lett.* **72**, 2757 (1994).
- [21] A. Damascelli, Z. Hussain, and Z.-X. Shen, *Rev. Mod. Phys.* **75**, 473 (2003).
- [22] A. Mans, I. Santoso, Y. Huang, W. K. Siu, S. Tavaddod, V. Arpiainen, M. Lindroos, H. Berger, V. N. Strocov, M. Shi, L. Patthey, and M. S. Golden, *Phys. Rev. Lett.* **96**, 107007 (2006).
- [23] J. D. Axe, A. H. Moudden, D. Hohlwein, D. E. Cox, K. M. Mohanty, A. R. Moodenbaugh, and Y. Xu, *Phys. Rev. Lett.* **62**, 2751 (1989).
- [24] T. R. Thurston, R. J. Birgeneau, D. R. Gabbe, H. P. Janssen, M. A. Kastner, P. J. Picone, N. W. Preyer, J. D. Axe, P. B ni, G. Shirane, M. Sato, K. Fukuda, and S. Shamoto, *Phys. Rev. B* **39**, 4327 (1989).
- [25] H. Kimura, K. Hirota, C.-H. Lee, K. Yamada, and G. Shirane, *J. Phys. Soc. Jpn.* **69**, 851 (2000).
- [26] V. N. Strocov, R. Claessen, and P. Blaha, *Phys. Rev. B* **68**, 144509 (2003).
- [27] C. J. Halboth and W. Metzner, *Phys. Rev. Lett.* **85**, 5162 (2000).
- [28] J. Gonz lez, *Phys. Rev. B* **63**, 045114 (2001).
- [29] H.-H. Wu, M. Buchholz, C. Trabant, C. F. Chang, A. C. Komarek, F. Heigl, M. v. Zimmermann, M. Cwik, F. Nakamura, M. Braden, and C. Sch b ler-Langeheine, *Nat. Commun.* **3**, 1023 (2012).